

# We are IntechOpen, the world's leading publisher of Open Access books Built by scientists, for scientists

6,900

Open access books available

186,000

International authors and editors

200M

Downloads

Our authors are among the

154

Countries delivered to

TOP 1%

most cited scientists

12.2%

Contributors from top 500 universities



WEB OF SCIENCE™

Selection of our books indexed in the Book Citation Index  
in Web of Science™ Core Collection (BKCI)

Interested in publishing with us?  
Contact [book.department@intechopen.com](mailto:book.department@intechopen.com)

Numbers displayed above are based on latest data collected.  
For more information visit [www.intechopen.com](http://www.intechopen.com)



---

# **Quantifying Stress in Crabs and Humans using Modified DFA**

---

Toru Yazawa

Additional information is available at the end of the chapter

<http://dx.doi.org/10.5772/59718>

---

## **1. Introduction**

Stress, which can be acute or chronic, is a term that has not been strictly defined, especially in the field of neuroscience. Scientists have not yet fully characterized the complete set of neuronal mechanisms that can explain stress. In this article, however, I use the term “stress” because it is the most appropriate one.

Stress is a physiological reaction of an organism to an uncomfortable or unfamiliar physical or psychological stimulus. Stress-inducing stimuli trigger reflex behavior, which results from alteration in the activity of the autonomic nervous system (ANS) and hormones. Reflex behavior includes a heightened state of alertness and increased heart rate. Acute stress is a short-term response that lasts for seconds, minutes, or days. In this article, “stress” refers to acute stress.

Scientists have not yet determined a method that can efficiently quantify stress. In fact, scientists have difficulty objectively defining whether an organism is expressing stress in response to stimuli. Through studies of crustacean hearts using electrophysiological methods, I have discovered that stressful and non-stressful states can be distinguished by heartbeat recordings: i.e., via electrocardiograms (EKGs). The methods used to measure stress in model animals can be applied to humans because model animals and humans are fundamentally similar in terms of autonomic nerve physiology. The autonomic cardio-regulatory function can simply be described as the combined action of acceleration and inhibition. In this article, I present empirical results of stress observations in both model animals and humans. The presented data provide convincing evidence that stress can be quantified.

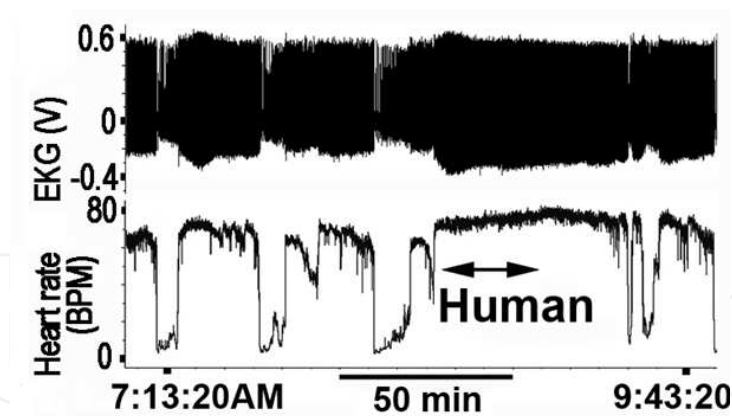
## 2. Brief history of crustacean heart physiology

Cardiac nerves—comprising accelerator nerves (CA) and inhibitory nerves (CI)—govern the activity of the heart in an involuntary manner in both model animals and humans. CA and CI are cardiovascular components of the ANS that transmit psychological information to the heart. Alterations in the activity of these neurons can modulate momentary heart rate and contractile force in a reflex manner in crustaceans as shown in Figures 1–3. Because the degree of stress can be measured by monitoring heart rate variability, the heart can be called a reflection of the neural activity of an animal.

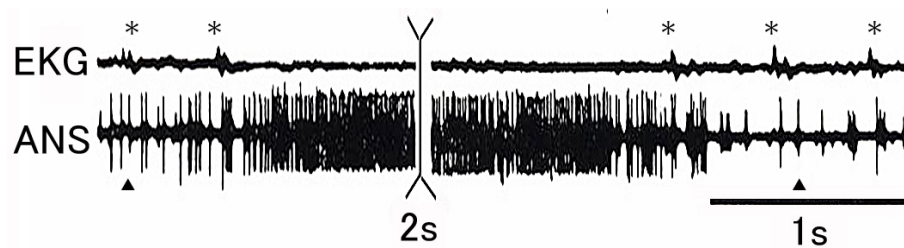
However, the cardiac regulatory function of the human ANS is not clearly understood because of the difficulty associated with recording ANS activity. Nevertheless, I have successfully recorded ANS activity in crustaceans. Both CA and CI are active when the heart is beating. This is evident in *in situ* recordings of nerve activity in hermit crabs in the 1970s (Figure 1, unpublished data). In decapod crustaceans, only one pair of nerves, termed the cardiac or regulator nerves, innervate the heart bilaterally. The crustacean system therefore appears simpler than the human cardiac nervous system. However, appearances can be deceiving: the fundamental mechanisms of the acceleration/inhibition functions are similar in humans and crustaceans, and the ANS controls the cardiac region in both animals. It is evident in Figure 1 that three different impulses varying in size indicate discharging: small (not marked), medium (shown by triangles), and large (not marked) impulses. A significant feature of Figure 1 is that the crab's heartbeat stopped completely during the period when the large-sized impulses were active, which is shown by a train discharge at a high frequency of approximately 50 or 60 Hz. Based on these observations, I was able to identify the neurons (in this case, the large-sized impulses) that transmit inhibitory commands. CI and CA always function in balance with each other. Figure 1 shows that the ANS dynamically controls the heart.

Healthy human hearts do not stop beating; only the rate of the heartbeat changes. However, crustacean hearts can cease beating for a period of time (Figure 2). A key finding in my crustacean study was that specimens showed a pattern of intermittent heartbeat cessation under healthy, normal, non-stressed conditions. The cessation was induced by an intermittent burst discharge of CI as mentioned above (Figure 1). An important observation was that the presence of a human caused interruptions in this intermittency. In other words, stress from an approaching human caused an alteration in ANS function: i.e., the intermittent pattern changed to a continuous pattern [2] (Figure 3).

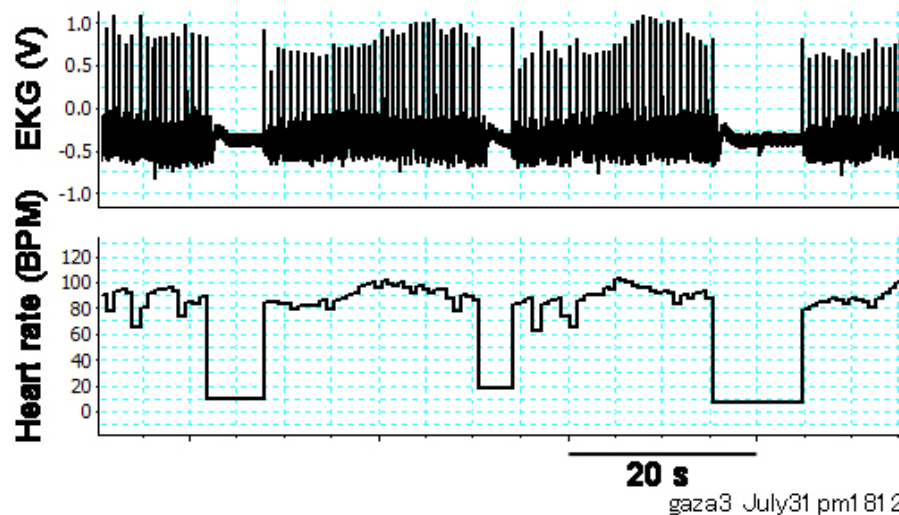
This intermittency was actually documented in the 1970s by Canadian crustacean heart researchers, J. L. Wilkens and B. McMahon, though they did not mention the role played by stress. (They found a strong relationship between cardiac and respiratory control.) The physiology of the crustacean ANS has been studied throughout the 20<sup>th</sup> century by Carlson (1900s), Alexandrowicz (1930s), Maynard (1950s, 1960s), Young [3], Field and Larimer [4], and Yazawa and Kuwasawa [5]. However, these authors did not provide information on the relationship between heartbeat and behavior of crustaceans.



**Figure 3.** Intermittent heartbeat cessation of a Japanese spiny lobster (*Panulirus japonicus*) was interrupted by an approaching human shown in an EKG recording from a live specimen.



**Figure 1.** Simultaneous recording of heartbeat (EKG) and cardiac nerve activity (ANS) of the hermit crab (*Dardanus crassimanus*). Asterisks (\*) indicate heartbeats.



**Figure 2.** Intermittent cessation of heartbeat shown in an EKG recording from a live saw tooth Gazami crab (*Scylla serrata*) specimen.

In summary, I recorded impulses of the cardiac nerves of crustacean hearts. I observed that CI discharged a burst of impulses at a high-rate, ~60 Hz, and concomitantly, CA momentarily

ceased their impulse discharge [1]. During the CI burst period, the heart rate disappeared or decreased significantly, although a rapid restitution of heartbeats occurred within one second. These brief cessations of heartbeats occurred intermittently and somewhat regularly during “stress-free” periods, for example, when the animal was hiding in a shelter. In contrast, the stress-free behavior was not exhibited if the lobsters or crabs were approached by humans. This response can be likened to the way cicadas stop singing when humans are in close proximity. These findings suggest that crustaceans are incredible specimens because their stress can be detected by electrocardiograms.

Crustacean and human hearts strongly resemble each other in structure and function. It is known that homologous genes (e.g., *Nkx2-5*, the NK2 homeobox gene) function to form the developing heart of all animals: [6]. In crustaceans and humans, both CA and CI connect with the cardiac pacemaker cells, but CA further proceed to the ventricular muscles beyond the pacemaker cells. Why do CA control the entire heart? The answer is that CA–muscle connections can implement direct modulation of contractile force, whereas CI merely suppress rhythm [5]. The resemblance between crustacean and human indicates that some knowledge obtained from crustacean should be applicable to human. See Recent report by Fossat et al.

(1) P. Fossat et al. “Anxiety-like behavior in crayfish is controlled by serotonin.” *Science* 344, 1293–1297 (2014).

(2) P. FOSSAT et al. “Anxiety-like behavior in crayfish is controlled by serotonin.” Society for Neuroscience, Poster 655.18/UU43 - Motivation and Emotions: Rodent Anxiety Models Tue, Nov 18, 1:00 - 5:00 PM 2014 Washington DC.

(3) OUTSIDE JEB. *The Journal of Experimental Biology* (2014) 217, 3389-3391

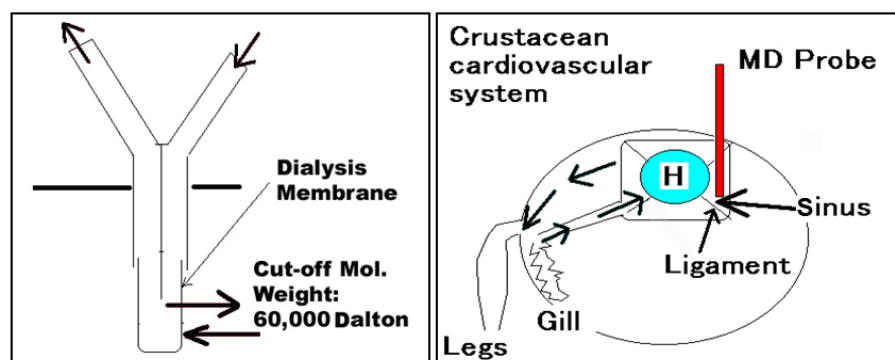
I studied electrocardiograms (EKG) of both animal models and humans and used modified Detrended Fluctuation Analysis (mDFA) to calculate the scaling exponent (SI) (originally, Peng et al., [7]). In this article, I show that the SI numerically is capable of distinguishing between healthy and unhealthy hearts, and between “stressed” and “relaxed” hearts. Further, I propose the mDFA to be a viable potential method for health/stress checking if incorporated into a device that can quantify stress through EKGs.

### 3. Electrophysiology method

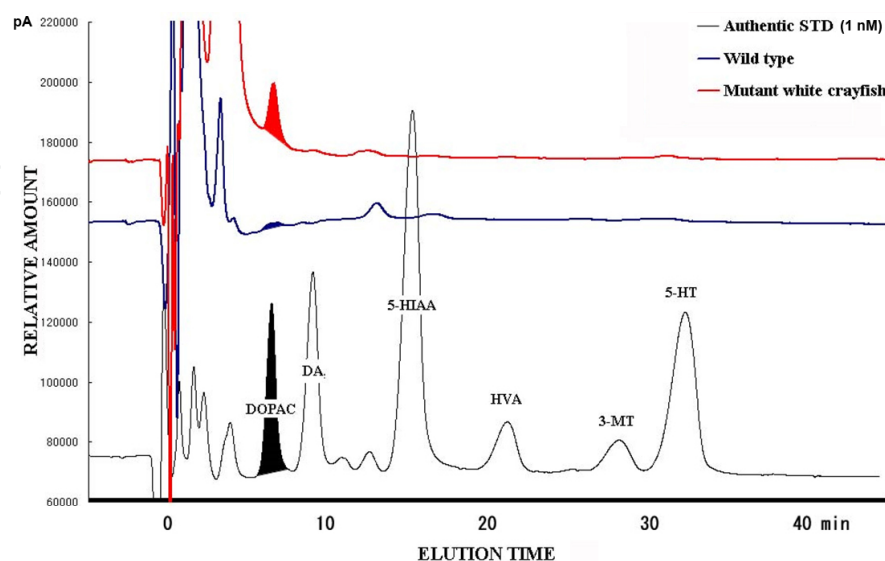
Human heartbeats were recorded using a PowerLab system (AD Instruments, Australia). A set of three, ready-made Ag–AgCl electrodes (Vitrode V, Nihonkoden Co. Ltd. Tokyo) were used for EKG monitoring. Permanently mounted metal electrodes were glued on the crustacean carapace for EKG recordings. These EKG signals were transferred to the PowerLab system and PC. All subjects were treated according to the ethical regulations of Tokyo Metropolitan University.

## 4. Stress hormone measurement

The stress response of the lobster to approach by a human (Figure 3) may involve the contribution of stress hormones, but combined hormone and EKG measurements have not been conducted. Therefore, I conducted micro-dialysis blood hormone measurements to determine whether hormones are involved in crustacean stress responses. I prepared four different HPLC-ECD (high performance liquid chromatography with electrochemical detection) machines. These machines were respectively set up to separate biogenic monoamines (dopamine, adrenaline, serotonin and their breakdown products), acetylcholine and related substances, amino acid neurotransmitters (glutamate, GABA, etc.), and peptide hormones. Blood samples were collected using a micro-dialysis probe for all HPLC analyses (Figure 4).

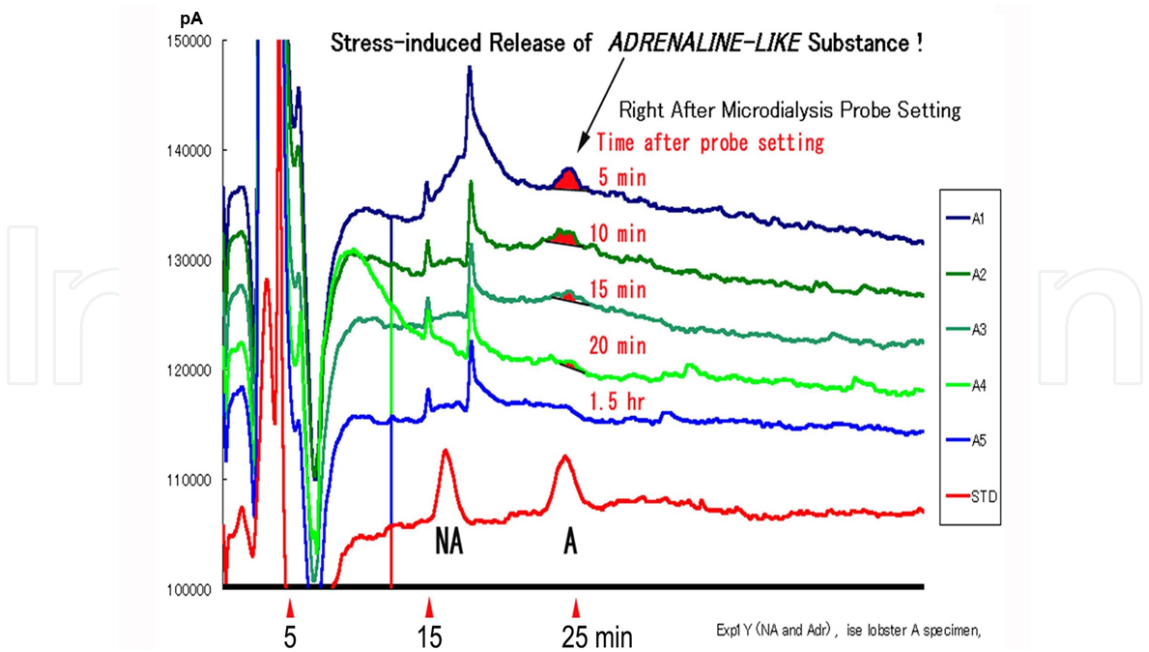


**Figure 4.** The micro-dialysis (MD) probe placed on the dorsal carapace of lobsters (left panel). The tip of the MD probe placed in the blood stream (right panel). H represents the heart chamber and arrows indicate the direction of flow.

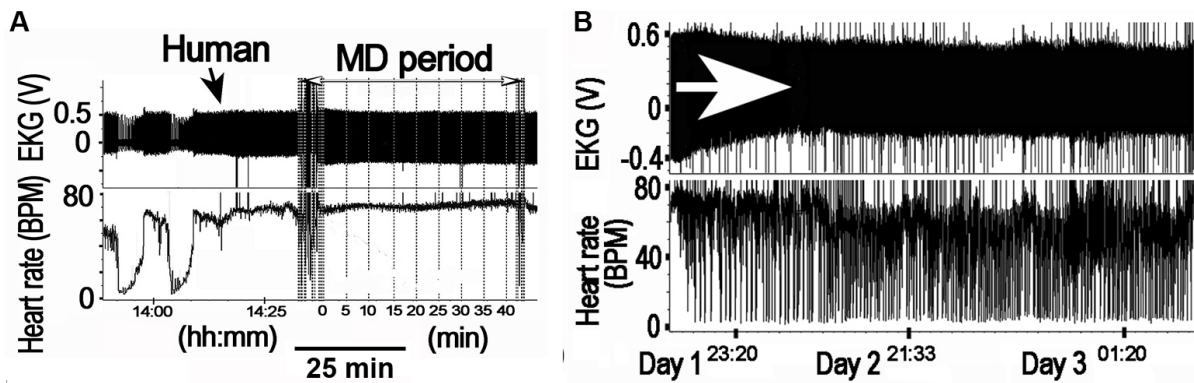


**Figure 5.** HPLC chart indicating the detection of DOPAC (a breakdown product of dopamine) using the HPLC system in a blood sample collected from a crayfish (*Procambarus clarkii*) specimen.



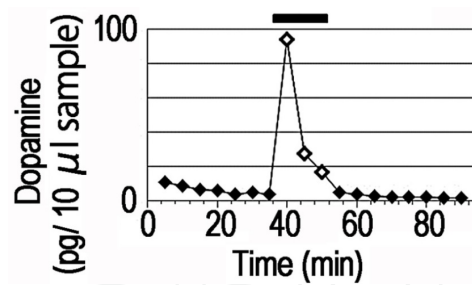


**Figure 6.** HPLC chart indicating the detection of adrenaline (A) in a Japanese lobster (*Panulirus japonicus*) specimen. Adrenaline release was induced by stress from human handling. Very little adrenaline was detected 20 min and 1.5 hour after the stress stimulus. Therefore, the adrenaline content measured at these times indicates the basal adrenaline content in the blood. Note: noradrenaline (NA) was not detected.



**Figure 7.** EKG recording and MD experiment in a Japanese spiny lobster (*Panulirus japonicus*). A, a human approached the lobster tank and conducted an MD experiment. B, continuous recording from A (note: the time scale is different).

Micro-dialysis HPLC (MD-HPLC) analysis detected a few substances in the blood samples before, during, and after stress stimulation. EKGs were continuously recorded to check stress responses. Figure 7 shows a lobster's response to a human, observed through EKG recordings. Significant features are evident in Figure 7. First, approach by a human interrupted the slow, repetitive heartbeat pattern (Figure 7A). Second, the micro-dialysis experiment resulted in continuous stress to the animal (MD period in Figure 7A). Third, the stressful reaction lasted for approximately one day, the period shown by a white arrow (Figure 7B).



**Figure 8.** Micro-dialysis HPLC detection of dopamine in a Japanese spiny lobster (*Panulirus japonicus*) specimen. The bar indicates a stimulation period of 15 min.

Figure 8 shows the stress-induced release of dopamine. Blood samples were collected for 5 min and collection vials were exchanged every 5 min by an automatic solution-sampling machine. A human entered the room containing the lobster for only a short time period (15 min); this period is indicated by the black bar. The human presence evidently irritated the lobster, triggering a sharp increase in dopamine concentration, but this was followed by a rapid decrease even though the stimulus was maintained for 15 min. The same stimulus also induced adrenaline release, shown in Figure 6. The detection of stress-related hormones was confined to dopamine and adrenaline and the breakdown product DOPAC. No other hormones that directly correlated with stress behavior were detected—e.g., serotonin, noradrenaline, amino acid neurotransmitters, and peptide hormones. Further details about these experiments can be found in [8].

A characteristic feature revealed by the MD-HPLC experiments was that increased levels of stress hormones are not maintained at a consistently high level even though the stress stimulation was steadily maintained for 15 min (Figure 8). In conclusion, acute stress is governed mainly by the functioning of the nervous system, whereas chronic stress more likely relates to hormonal systems. Hormone release seems to be able to trigger a chain reaction in biochemical pathways that results in a state of chronic stress.

Based on the results of the MD-HPLC examinations, I suggest that stress can be quantified by measuring heartbeat rather than hormones. Stress can be determined using heartbeat fluctuation analysis; the method used was modified DFA (mDFA).

## 5. Modified DFA and DFA

In this article, I compare the methodologies of original and modified DFA. While most of the computation sequences in DFA and mDFA are similar, there is one difference in the computation process.

In DFA and mDFA, the scaling exponent (Peng used the Greek letter alpha) or scaling index (SI) is calculated from time series data that obey the scaling law. Here, I use SI to refer to both.

In the mid-1980s, Goldberger pioneered the application of nonlinear dynamics to clinical cardiology [9]. Thereafter, a voluminous literature appeared on chaos and nonlinear analysis



in the life sciences [10]. The following literature provides information on nonlinear physics with respect to heart physiology and DFA: Peng [11], Glass [12], Stadnitski [13], Stanley [14], Goldberger [9], Katsuyama [15], Pérez [16], Liebovitch [17], Huikuri [18], Bigger [19], Scafetta [20], and other work cited in these references. In addition, the scaling exponent, DFA, and topics related to fractality research, for example, fractal, scaling, the Hurst exponent, and power spectral density, are well explained by T. Stadnitski [13]. DFA is based on the concepts of scaling and self-similarity [13]. Peng's DFA [7] deals with critical phenomena. (Details of the mathematics of DFA can be referenced elsewhere [9-19]). One DFA program, PhisoNet, provided by Goldberger, Peng and others is available on the internet. However, there is no web-based mDFA program available. Regardless, an mDFA program can be written with an understanding of DFA and programming skills (I am a biologist and received programming support from a graduate student, Katsunori Tanaka, who constructed an mDFA program under my supervision using C++programming language).

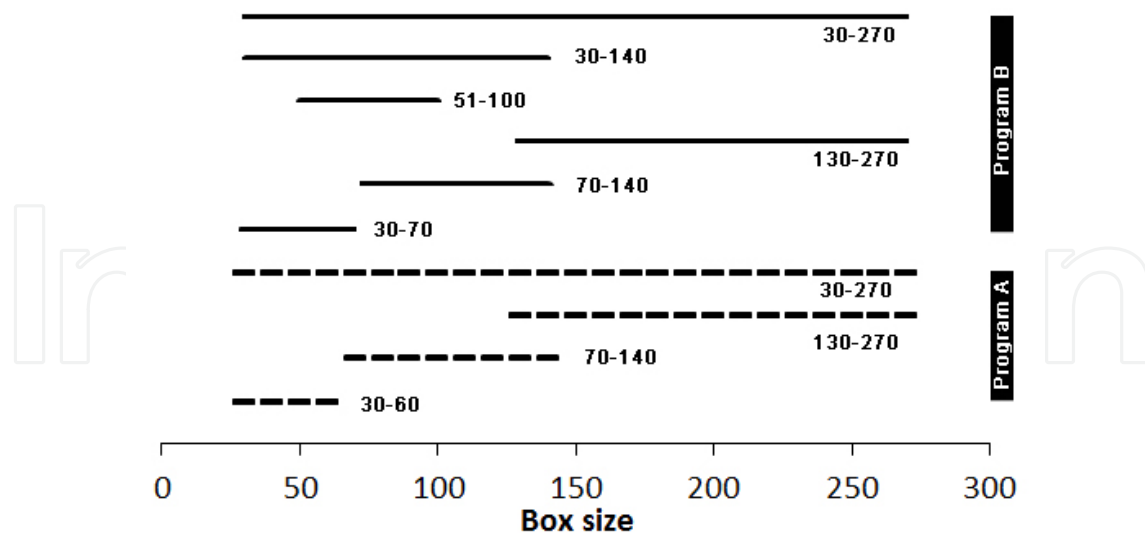
While the genesis of DFA was long ago, no one has since constructed a useful device/instrument to quantify stress using it. In this article, I argue that implementing power law concepts in DFA is a superior method for its practical use in biomedicine. In addition, I present the results of our mDFA applied to real-world data. I anticipate that this literature will initiate a public debate on whether to construct such a device/instrument, and hope that a functional DFA device will be constructed as a result. This work is being performed in collaboration with Symphodia Phil Confidential, Japan (President O. Takiguchi). Empirical data and the device concept were previously presented at a conference of the Society for Chaos Theory in Psychology and Life Sciences in Milwaukee, Wisconsin, USA (August 2, 2014).

Although DFA is not a recent development, the technique is somewhat difficult to understand. An important concept of DFA is that if data exhibit scaling characteristics and self-similar fluctuations [11, 14], recorded signals and their magnified/contracted copies are statistically similar. In general, statistical parameters such as the average and variance of fluctuating signals can be calculated by taking the average and corresponding variance of the signals across a certain section. In DFA and mDFA, however, the average is the squared average of the data. The calculation of the statistical parameter thus depends on the size of the section.

To use DFA as a practical tool for instantaneous determination of heart condition, the appropriate section size, i.e. box size or number of heartbeats, needs to be determined. A practical DFA tool should NOT be subject-specific. Rather, it should be constructed for general use across the population. The section size, which is a restricted period of time, was determined to range from 30 to 270 beats after conducting hundreds of tests.

## 6. EKG recording before mDFA

mDFA requires accurate heartbeat interval measurements without missing a single heartbeat. Stable EKG recordings are needed for accurate detection of peaks in the data. If subjects move (e.g., talk, touch, walk, squat, exercise, etc.) commercially available medical-EKG machines are



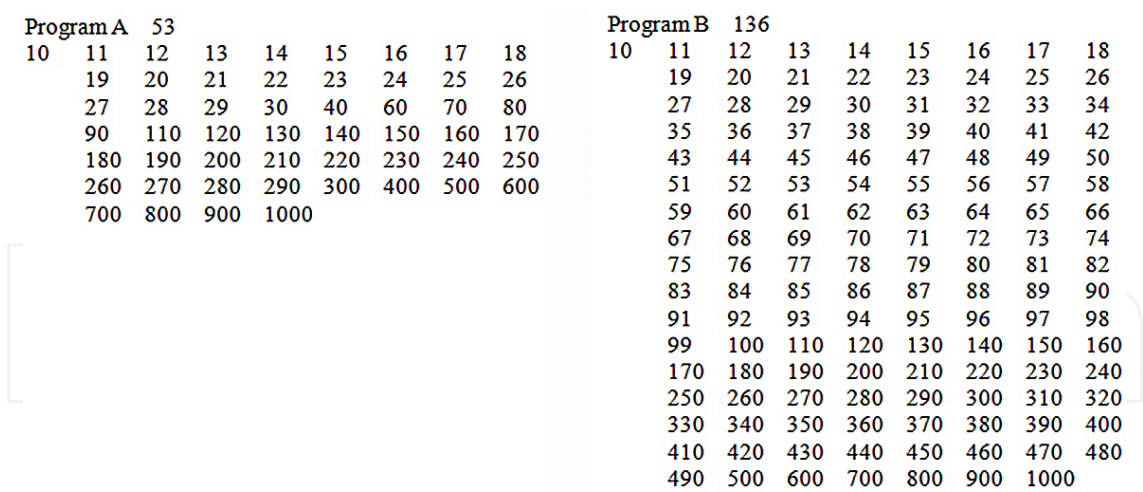
**Figure 9.** Range in box sizes used for mDFA (i.e., the slope from one particular box size to another).

not reliable because the EKG trace is frequently lost from the recorder chart or screen under these conditions. Accurate identification of peak heartbeat times were a necessary condition in this study. Therefore, I constructed a baseline-stable EKG recording amplifier with an input time constant of 0.1 or 0.22 s ( $C=0.1 \mu\text{F}$ ,  $R=1 \text{ M}\Omega$ , or  $C=0.22 \mu\text{F}$ ,  $R=1 \text{ M}\Omega$ , respectively) and amplification-gain of 2000 times. This made it possible to record baseline-stable EKGs. I used a 1-kHz sampling rate. Based on my own electro-physiological observations, I knew that the peak time of an action-potential always fluctuates in the order of milliseconds in response to a stimulus. Therefore, I used a 1-kHz sampling rate (1000 dots per 1000 milliseconds). After detecting peak heartbeat intervals, I constructed an inter-heartbeat interval time series (such as the R-R peak interval of conventional medical EKGs). This time series was analyzed using the mDFA program.

To conduct mDFA and obtain reliable scaling exponent (SI) values, a recording of ~2000 consecutive heartbeats was required; this number was used throughout my research. If a dataset contained 4000 or 5000 heartbeats, these were divided into two data sets. The ideal (minimum essential) number of heartbeats for use in an mDFA instrument would be ~2000. In fact, various data lengths of EKGs, ranging from 700 to 5000 heartbeats are used. In this article, analysis based on 2000 beats as well as shorter and/or longer data lengths are presented in some figures. To obtain stable results in a practical health-determining device, a 30-min EKG recording is ideal (here, 1900–2100 beats were used).

There are several ways to detect heartbeat timing; however, I prefer stable baseline EKGs. In terms of a stable baseline, short and constant EKG recordings are superior to finger pulse and light-sensor (infrared) blood flow recordings. However, consecutive R-R intervals of ~2000 beats are required irrespective of the type of recording used.

Several mDFA computations were performed simultaneously: scaling exponents in various box sizes were computed (Figure 9). Initially (from 2004 to 2006), program A was used, which



**Figure 10.** Box size (number of heartbeats) for the mDFA programs. Program A and Program B contained 53 and 136 boxes, respectively. Programming language C++.

included box-ranges [30: 60], [70: 140], [130: 270], and [30: 270]. These four ranges were automatically and simultaneously computed. However, any box size range could be manually computed if necessary. Then, program B was added in 2006, which included box-ranges [30: 70], [70; 140], [130: 270], [51; 100], [30; 140], [30; 270] (Figure 9). These automatic ranges were arbitrarily determined. Until now, programs A and B have been used simultaneously. All existing EKG-mDFA results were computed using both programs.

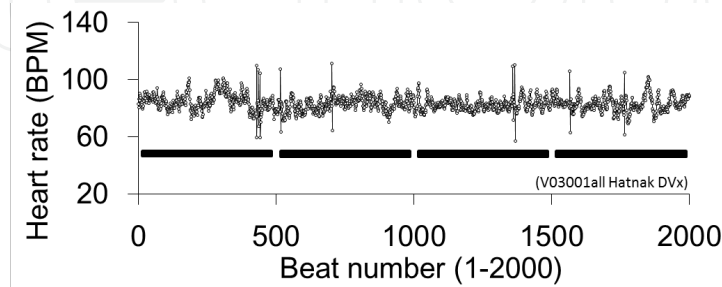
Program A computed 53 box points and program B computed 136 box points (Figure 10). This increase in box number occurred because of an increase in the PC calculation speed due to a Windows software improvement. A device requires relatively rapid computation of the scaling exponent. An average scaling exponent was computed in each computation, calculated as the average of the scaling exponents across the range of box sizes (see Figure 22 and 23).

mDFA calculations use recordings of approximately 2000 beats, digital recordings at a 1-KHz sampling ratio, and a box size range of [30: 270] in the following sections of this article, unless otherwise mentioned.

## 7. Box size

The mDFA program generated by K. Tanaka was based on an article by Scafetta and Grigolini published in 2002 [20]. These authors pointed out that DFA does not reliably detect the distribution of the Lévy time series [20]. The mDFA program is intended to observe the scaling behavior over a wide range of SI values. DFA focuses on critical phenomena and an SI value near 1.0, which is a Gauss distribution time series. In the current study, there were significant differences in the computation results between the mDFA and Peng’s DFA, especially when diseased hearts were examined. If mDFA was used instead of DFA, diseased hearts exhibited a high SI (SI≈1.4, Table 1).

The idea of using a box in mDFA (and DFA) computations is presented in Figure 11 for 2000-heartbeat interval time series obtained from a human subject. Seven clear irregular beats are evident, i.e., so-called premature ventral contractions (PVCs) or ectopic heartbeat. The four black bars indicate that the 2000-beat data set was divided into four boxes. Here, there are 500 beats in each box; therefore, the box size is 500. Every box always has an identical number of beats in any mDFA/DFA computation. In mDFA (not DFA) computations using a PC, the box size is changed cyclically from 10 to 1000 as shown in Figure 10.

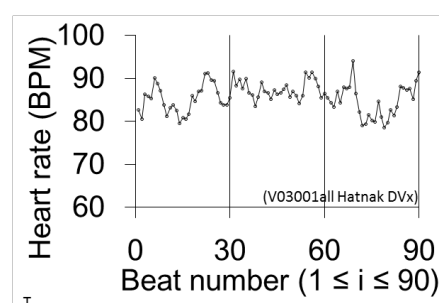


**Figure 11.** Interval time series and boxes.

## 8. Arithmetic calculation and detrended data

Here, the mDFA procedures are briefly shown. First, one can obtain heartbeat interval time series  $\{X_i\}$  and construct a “box” (Figure 12). Second, average heart rate  $\langle X \rangle$  is computed (Figure 13). Third, the values  $X_i - \langle X \rangle$  are computed (Figure 14). All data fluctuate around the zero line (see Figure 14).

Next, an integrated series (sigma) of all data fluctuating around the zero line  $q_i = \sum_{k=1}^i (x_k - \langle x \rangle)$  can be obtained (Figure 15). Note the random walk-like steps. A regression line is computed for each box using a fourth order (biquadratic) polynomial (data not shown) (Figure 16). Then, the procedure is detrended by computing  $s_i = q_i - q_j$  (Figure 17).



**Figure 12.** Heartbeat interval time series  $\{X_i\}$  and boxes. Ninety beats from 2000 beats are shown.

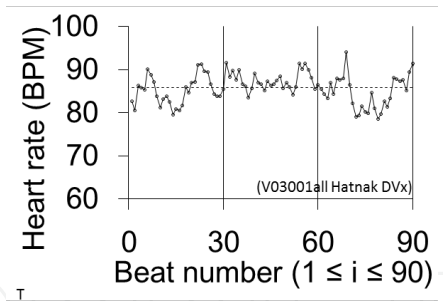


Figure 13. Average heart rate, i.e.,  $\langle X \rangle$ ; note the dotted horizontal line.

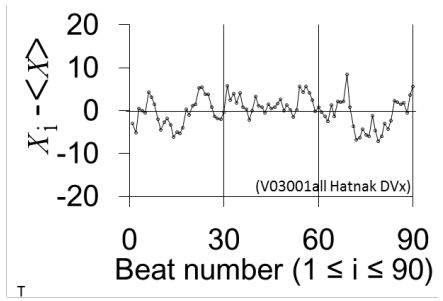


Figure 14. Average heart rate  $\langle X \rangle$  is deduced from  $\{X_i\}$ , resulting in a time series fluctuation around zero.

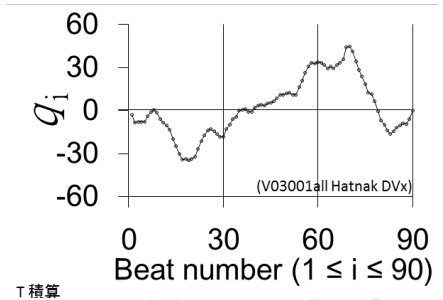


Figure 15. An integrated series,  $q_i$ .

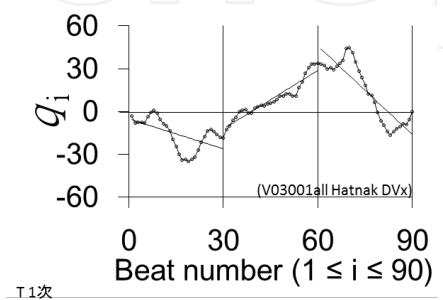
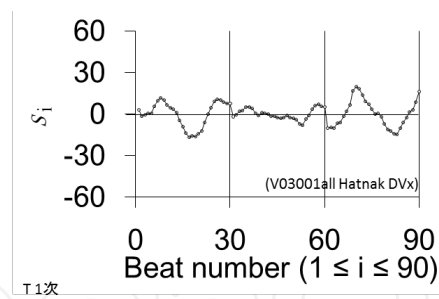
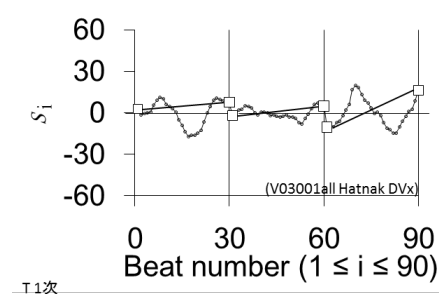


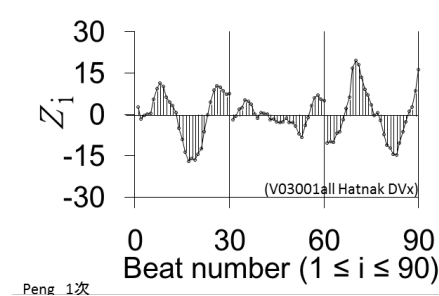
Figure 16. Regression lines,  $q_i$ .



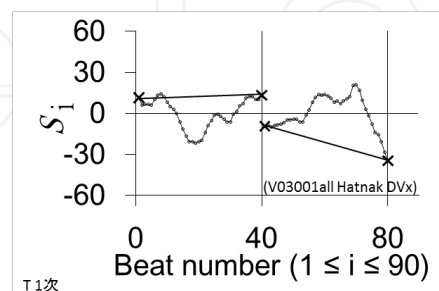
**Figure 17.** Explanation of detrended computations,  $s_i = q_i - q_j$ .



**Figure 18.** Computation of mDFA.



**Figure 19.** Peng's DFA showing the distance between each data point and the regression line.

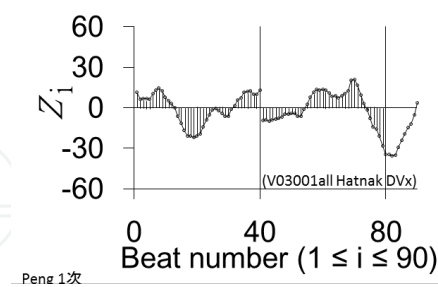


**Figure 20.** An example of mDFA with a box size of 40.

Then, in mDFA (not DFA), the program calculates how many steps proceeded after traveling within a box (Figure 18). This is an mDFA-exclusive computation, which is not used in Peng's DFA. Peng's DFA program calculates the distance ( $z_i$ ) between random walk-like lines ( $y_j$ ) and



regression lines ( $y_v$ ) (note the numerous vertical lines in Figure 19) as  $y_j - y_v$ . The data presented in Figure 20 and 21 represent differences between mDFA and DFA with a box size of 40.



**Figure 21.** An example of Peng's DFA with a box size of 40.

## 9. Scaling

Scaling graphs are constructed using the following procedures. The scaling exponent can be determined using an integrated series (Figure 15). The important variables are the number of boxes ( $N/n$ ), where box size ( $n$ ) and interval data number ( $N$ ) are given by the integrated series. The box size ( $n$ ) can be changed from 10 to 1000 in mDFA computations (see Figure 10). In addition, the variance,  $F(n)$  can be calculated for each box size ( $n$ ). Then, the following graphs can be drawn: Logarithm ( $n$ ) vs. Logarithm  $F(n)$ , and linear regression lines across various box sizes (see Figure 22). These procedures were used to compute the scaling exponent SI (or Greek letter alpha,  $\alpha$ ).

The equation used to determine the scaling exponent in Peng's DFA program (source code obtained from PhysioNet) is:

$$F(n) = \sqrt{\frac{\sum_{k=1}^N (y_k - y'_k)^2}{\frac{n}{N}}}, \quad (1)$$

where  $y_k$  is the integrated series and  $y'_k$  is the regression line.

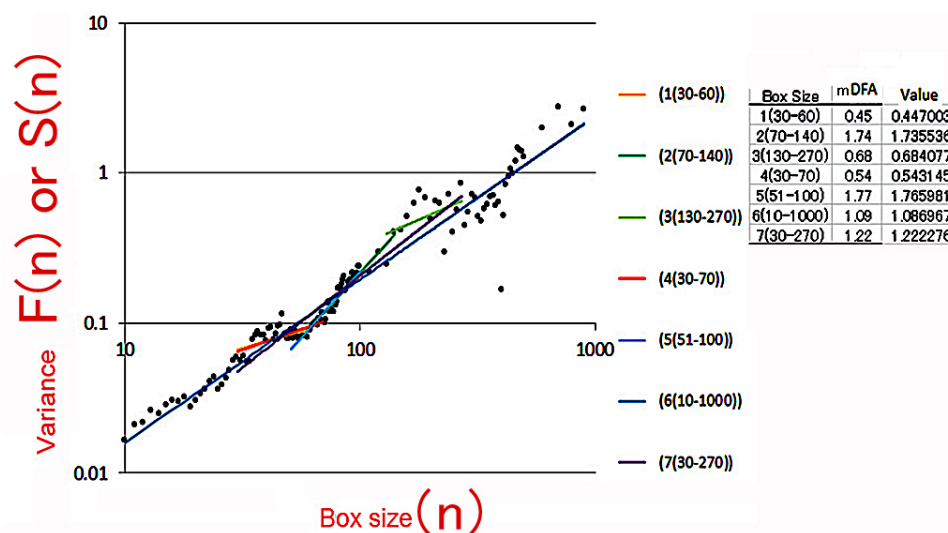
In the mDFA program, however, the following equation is used to determine the scaling exponent:

$$S(n) = \sqrt{\frac{\sum_{j=0}^{\frac{N}{n}-1} \{(q_{jn+n} - q'_{jn+n}) - (q_{jn+1} - q'_{jn+1})\}^2}{\frac{N}{n}}}, \quad (2)$$






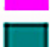
where  $F(n)$ ,  $S(n)$ ,  $q_i$  and  $q'_i$  are the same as Peng, but different letters are used for comparison between mDFA and DFA. Based on this equation, mDFA computations can be performed to determine the scaling exponents for practical use (see Figure 18 and Figure 20).

First, a graph of variance vs. box size (Figure 22) can be constructed, followed by determination of the scaling exponent (Figure 22 and Figure 23). For practical use of mDFA as a device, one can use the slope of [30: 270] because the value is nearly always close to the average value. This condition was applied to most of the empirical results presented below.

In summary, in Peng's DFA, the SI is calculated from the variance,  $\langle(x_i)^2\rangle$  and the random walk-like steps are considered. However, in the mDFA presented here, SI is calculated as  $\langle(x_{i+j} - x_i)^2\rangle$ . According to my physicist colleagues, the mDFA idea originates from a structure and function distribution and deals with scaling.



**Figure 22.** Determining SI in mDFA. Various SI values were computed simultaneously.

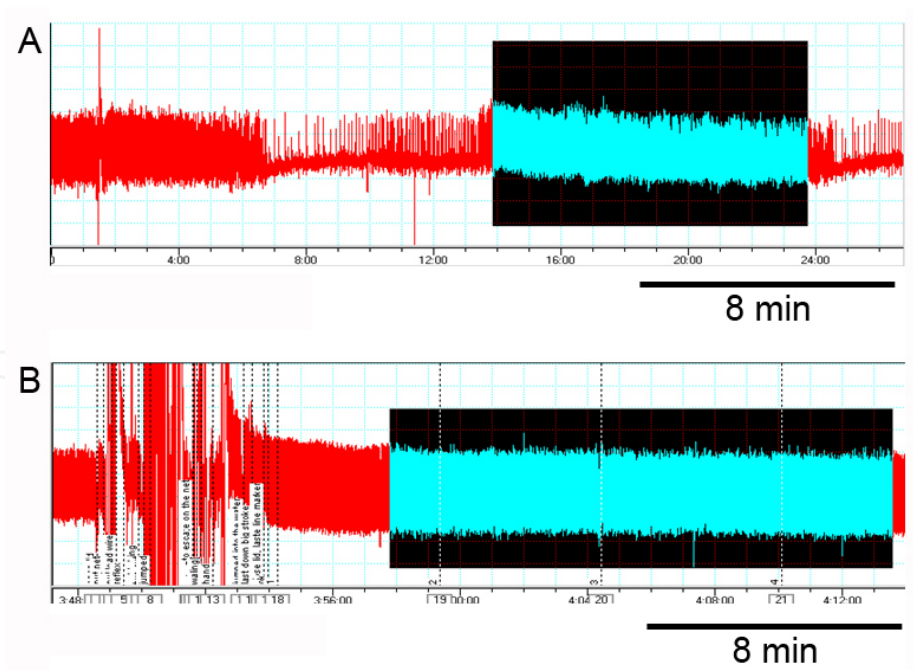
Box size	Scaling exponent	
30-70		1
70-140		0.71
130-270		1.21
51-100		0.75
30-140		0.91
30-270		0.98
AVE		0.92

**Figure 23.** Examples of SIs.

10. Stress quantification using mDFA

Lobster EKGs are presented in Figure 24. The data presented in Figure 24A were recorded when specimens were in a non-stressful state when no human was present in the room. The data presented in Figure 24B were recorded during micro-dialysis blood sampling. The heartbeat interval time series obtained from the highlighted section is shown in Figure 25 for 578 beats. Under the no-stress condition, the lobster exhibited a dynamically changing pattern (Figure 25, red line) indicated by numerous spikes in the data. This is evidence that the heart received an inhibitory command from CI. In contrast, the lobster under the MD stress condition did not exhibit such a dynamic pattern (Figure 25, black line). Inhibitory neural control was not evident, suggesting the stressed state is a state dominated by acceleratory neurons.

The scaling nature is expressed as a slope in the mDFA graph. The scaling nature of the no stress and MD stress states are presented in Figure 26. mDFA computation revealed a significant difference between the two states. Stress (caused by an approaching human) clearly decreased the slope (Figure 26 and 27). SI values of approximately 0.55 and 1.0 were obtained when a human did or did not approach the lobsters, respectively (Figure 27). These animal model experiments suggested that it may be possible to quantify human stress using the mDFA technique.



**Figure 24.** EKGs measured under no-stress (A) and MD-stress (B) conditions (these data were collected from the same lobster used in Figures 3 and 7).

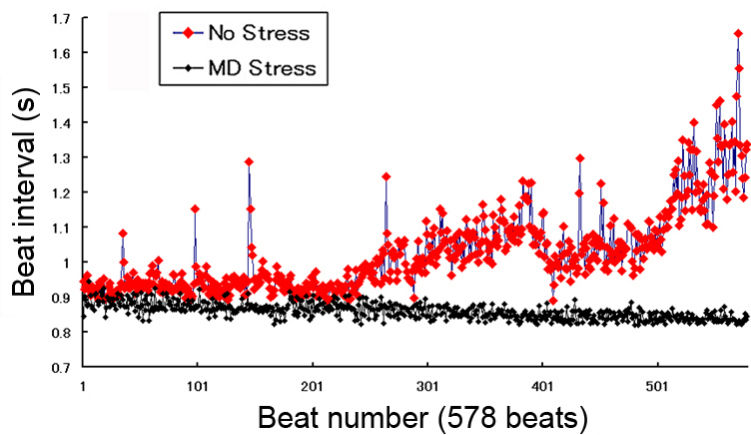


Figure 25. Interval time series obtained from data presented in Figure 24.

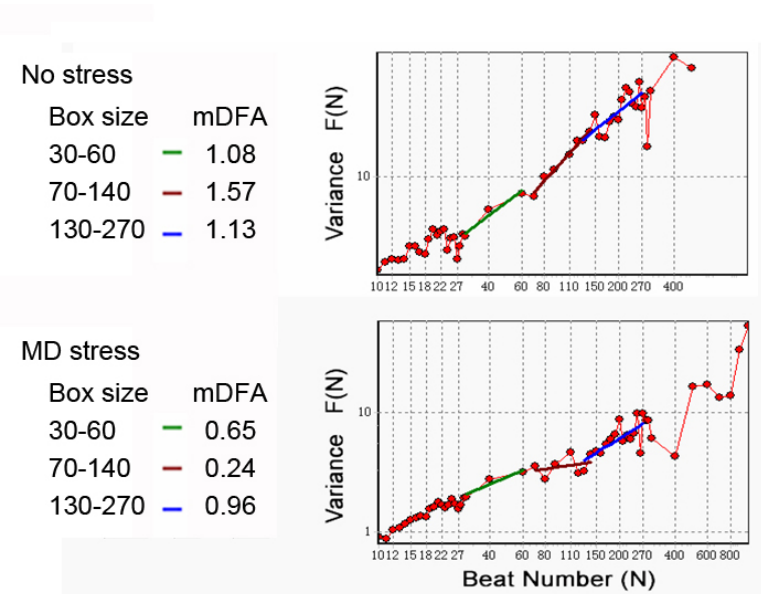


Figure 26. Results of mDFA (program A). Slope and SI for no-stress and MD stress conditions.

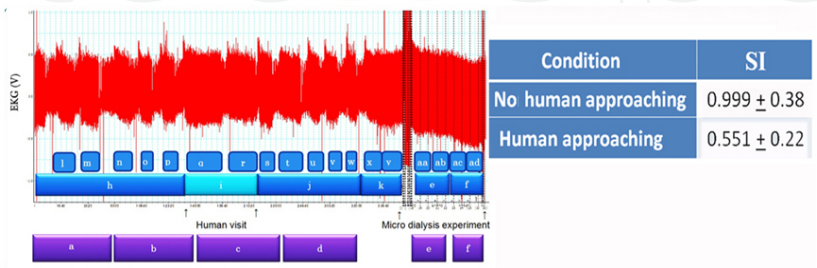


Figure 27. Scaling exponent (SI) computed from EKGs under no stress and MD stress conditions. SI computations from various time periods are shown by bars (a, b, c,---ac, ad).

## 11. Humans

Human EKGs were analyzed using mDFA. Table 1 indicates considerable differences in SI values between stressed and non-stressed individuals. Stress significantly lowers SI. mDFA revealed that the President and Dean of the University had low SIs, whereas teaching-only professors had healthy SIs close to 1.0.

The Appendix in Table 1 shows that heart muscle injury (such as myocardial cell damage caused by ischemia or heart operations) can be identified using mDFA. People with a poor medical history have high SIs, considerably higher than 1.0. It is possible that the hearts of patients who suffered from cardiac disease and recovered through successful medical treatment may have scar-like non-muscle tissue; i.e., a fibrous matrix or debris following necrosis. This tissue might cause abnormal fluctuation of heartbeats, which can be detected by mDFA. Although there is no mathematical explanation as to why the SI values are so high, it is notable that mDFA was able to distinguish ischemic hearts from healthy ones. It is remarkable that injured hearts have exceptionally high SIs. In fact, they echo previous findings of heart damage in crabs and lobsters that died suddenly during experimentation (Presented at international conferences: Yazawa et al. Neurodynamical Control of the Heart of Healthy and Dying Crustacean Animals. CCCT2005 Proceedings Vol. 1, pp. 367-372; Best Papers of IIIS Conference WMSCI 2006, DFA on Cardiac Rhythm: Fluctuation of the Heartbeat Interval Contains Useful Information for the Risk of Mortality in Both Animal Models and Humans)

Categories	Age	Stress level (Interview)	SI
Business owner (a company) No. 1	50s, Male	Fairly low	1.03
Business owner (a company) No. 2	50s, Male	High	0.72
Top management, President of a Univ.	60s, Male	High	0.84
Top management, Vice President of a Univ.	40s, Female	High	0.84
Middle management, Dean	40s, Male	High	0.72
Middle management, Secretary of president	40s, Female	High	0.76
Ordinary employee, Teaching only professor, No. 1	50s, Male	Fairly low	1
Ordinary employee, Teaching only professor, No. 2	50s, Female	Fairly low	0.98
Table 1. Appendix: Cardiac disease			
	Age	Daily life	SI
Patient with stent-placement	60, Male	OK	1.26
Patient with bypass-surgery	45, Male	OK	1.38
Patient with implantable cardioverter	53, Male	OK	1.22
Ventricular septal defect (20 y ago operation)	48, Female	OK	1.41
Healthy representative, housewife	46, Female	OK	1.03

**Table 1.** Comparizon: Stress level and exponent value (Indonesia, 2012, working with Prof. A. Hutapea

The SI data presented in Table 1 (and explained in Figure 28) show that mDFA is able to detect job-related stress. Some of the subjects presented in Figure 28 are the same as those shown in Table 1. Interestingly, the people who had administrative and teaching-professor obligations were somewhat serious during the EKG measurements and exhibited low scaling exponents. However, teaching-only professors who appeared happy (they laughed and spoke during the

EKG measurements) had healthy exponents with values near 1.0. It is likely that mDFA can quantify stress; however, additional empirical results on a greater number of samples are needed before a definite conclusion can be reached.

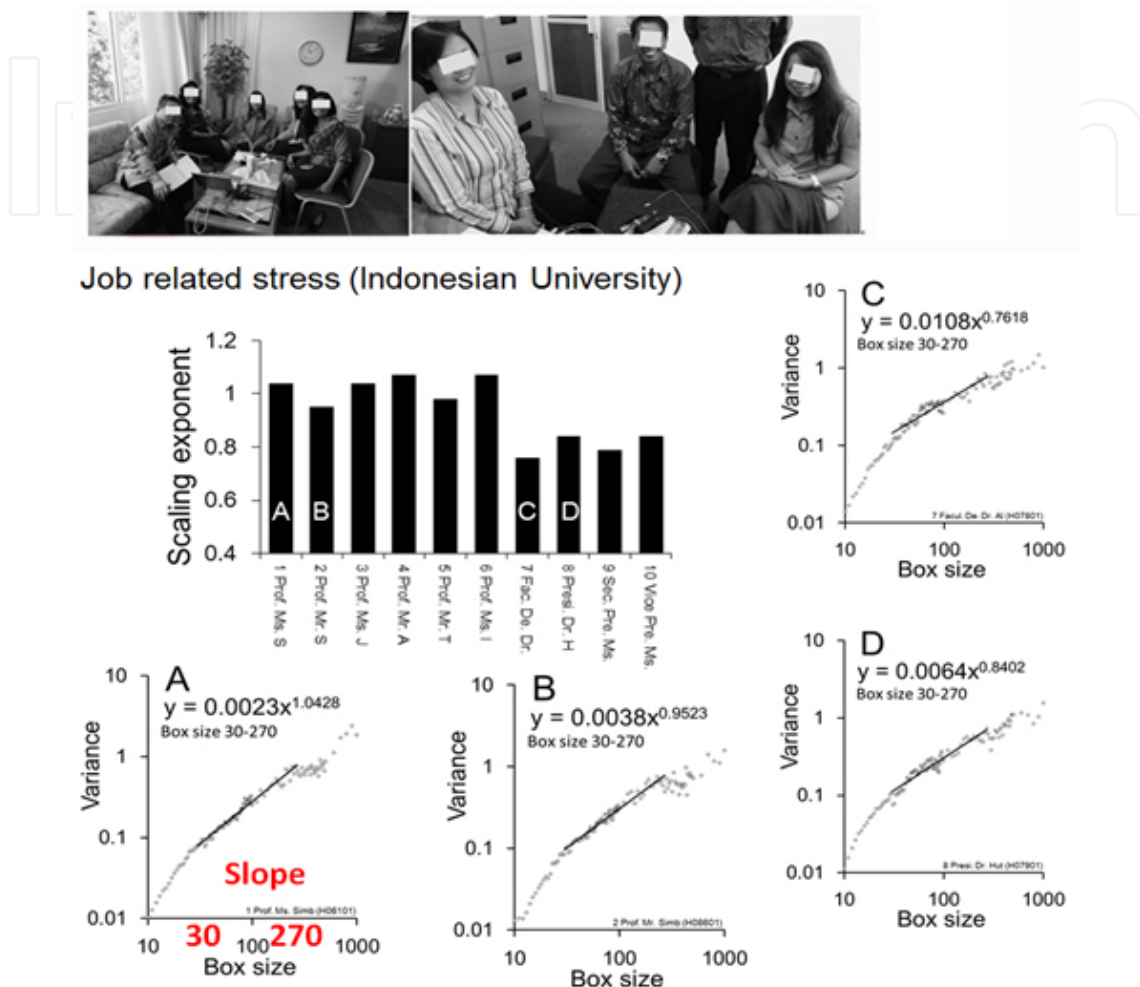


Figure 28. Job-related stress determined using mDFA (some are identical data shown in Table 1)

## 12. The heart reflects neural activity: Individual stories

A subject who volunteered for a long-term follow-up study had her EKG measured yearly under sitting and talking conditions, always on a September afternoon at approximately 3 PM. In 2006, she had a good SI and after that appeared normal in terms of mDFA. However, as can be seen in Figure 29, her SI changed dramatically over the years.

This subject did not disclose any personal issue until 2009 when she related that she experienced difficult conditions in her work place in 2007 and 2008 and wanted to relocate. In addition, she lost a loved one to illness in 2008 and left her office job at the end of 2009. Her



environment improved greatly by 2010; her EKG was not measured in 2011, and she had a good SI in 2012 (data not shown).

Another subject was caring for her aging mother at home (Figure 30). The caregiver did not sleep from 28–29 September because her mother did not sleep. Consequently, the subject’s SI was very low (3 PM on 29 September). However, she slept well the following two nights because her mother slept well. This subject visited my exhibition booth at Innovation Japan 2011.

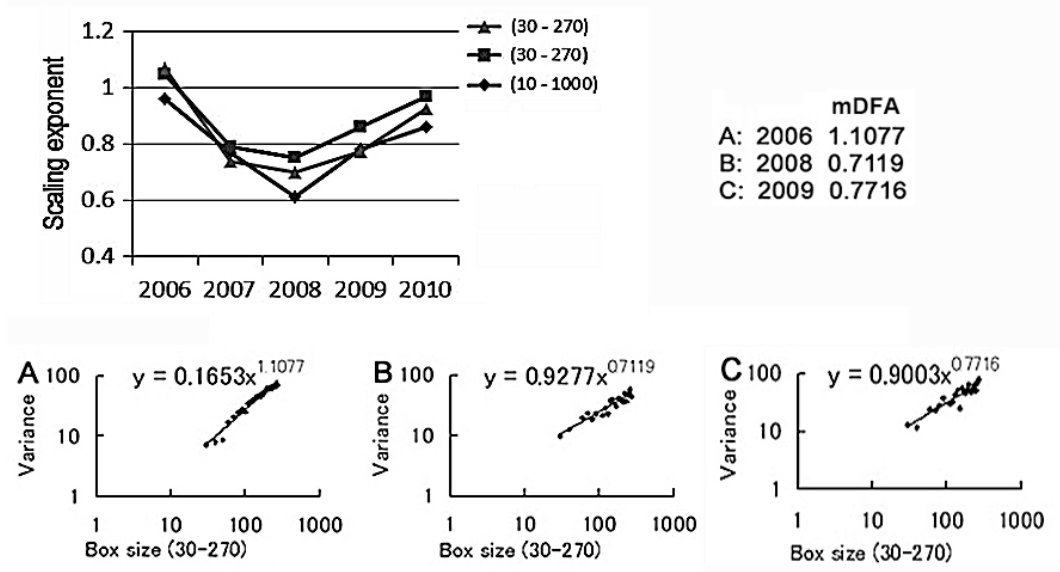


Figure 29. EKG data from a woman aged 27 years collected in September 2006 at 3 PM and five-year follow-up results.

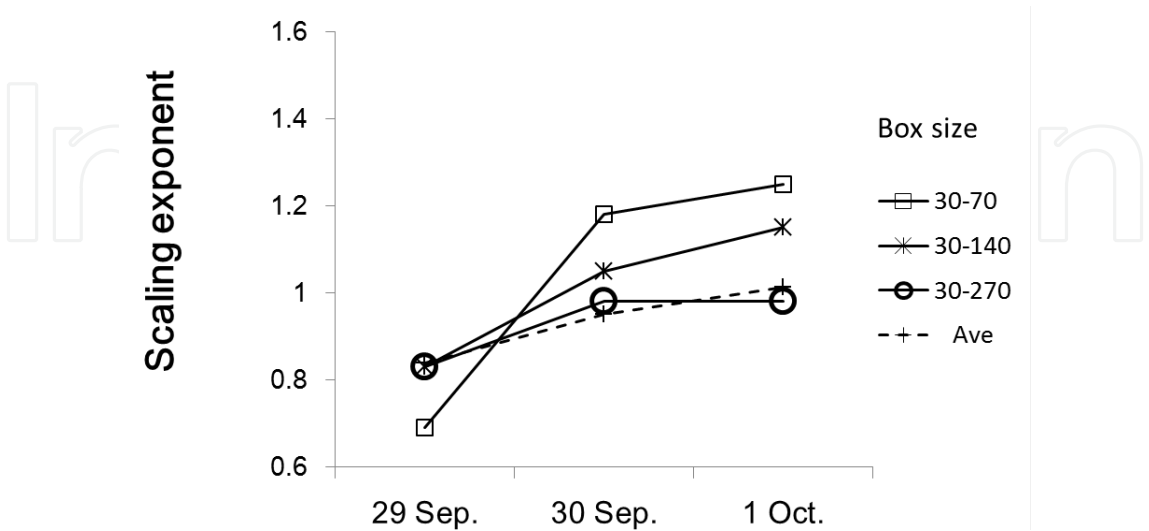
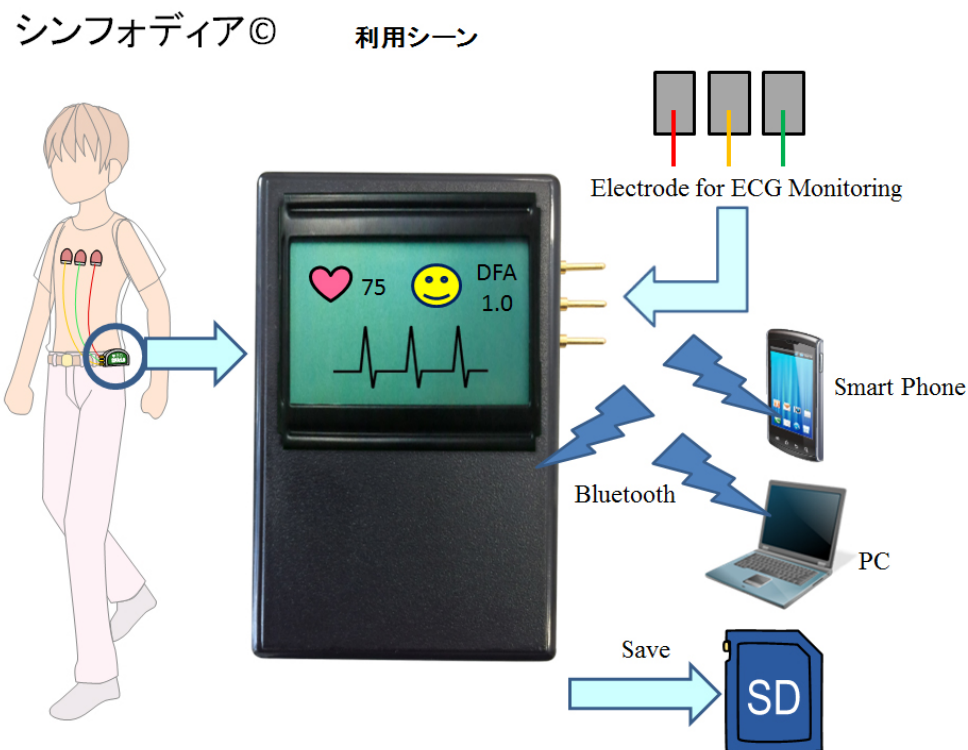


Figure 30. Sleep deprivation decreases SI. These data were collected from a woman in her 50s who was taking care of her aging mother.

### 13. A device

I am currently collaborating with a company to construct a device equipped with a stable-baseline (meaning, the EKG trace is NOT lost from the recorder chart or screen) EKG amplifier and data logger. In the future, an mDFA program will be incorporated into the device. The device will instantaneously compute SI, and EKG data, mDFA results, and SI values will be stored on an SD memory card. All data will be transmitted to a PC through a web-based system (Figure 31).



**Figure 31.** A device that records stable-baseline EKG (Symphodia Phil Confidential, Japan).

### 14. Discussion

Unique characteristics of mDFA are shown in Figure 18 and 20. In addition, the unique mDFA computation is specified in equation (2); DFA does not use this procedure.

mDFA calculates SI using a method that includes preparation of time series data, removing trends from the data, determining statistical variations, constructing a graph of  $F(n)$  vs.  $(n)$ , where  $F(n)$  is variance and  $(n)$  is box size, and determining the slope, i.e., SI. In order to

construct a gadget that rapidly calculates SI, I determined an appropriate scaling zone where a straight line and a regression line were drawn using the least-squares method; this zone is [30: 270] in beat per min (BPM).

Until now, a DFA-user must determine the box range before drawing a regression line to obtain the SI. I determined the best range to compute SI automatically is [30: 270]. Biological systems do not operate optimally because ranges that are too small or too large are avoided. As a biomedical tool, however, mDFA uses a special box-range [30: 270]. Currently, people can construct their own device to analyze their own cyclic phenomena. The device would automatically return SI values when people include time series data, and SI could be computed for any time series interval.

The time length of 270 heartbeats in the [30: 270] box range corresponds to 270 sec if the heart beats at a steady ratio of 60 BPM, which is equivalent to 3–4 min. This time length has a particular significance with respect to neuroscience, because internal biochemical reactions can retain a steady state for this length of time. I can wait for three minutes before instant noodles are cooked. A boxer fights with full power for three minutes. The neuron network functions under the three-minute law. Short-term memory and acute stress, for example, can last for three minutes but they can also decline after three min. The length [30: 270] (three min) could be a biologically important number.

## 15. Conclusion

mDFA and SI provide useful information. mDFA can be incorporated in the future into a device for checking health and stress levels. It is possible that anyone could construct their own mDFA program for developing such a device.

## Acknowledgements

This work was supported by JSPS Grants No. 23500524 and No. 2635050. I thank DVX Inc. Tokyo, Japan, for financial support for research, No. 4DQ404, for 2012, 2013, and 2014.

## Author details

Toru Yazawa\*

Address all correspondence to: [yazawa-tohru@tmu.ac.jp](mailto:yazawa-tohru@tmu.ac.jp)

Tokyo Metropolitan University, Japan

## References

- [1] T. Yazawa, K. Kuwasawa, Intrinsic and extrinsic neural and neurohumoral control of the decapod heart, *Experientia* 48 (1992) 834-840.
- [2] T. Yazawa, T. Katsuyama, Spontaneous and repetitive cardiac slowdown in the freely moving spiny lobster, *Panulirus japonicus*, *Journal of Comparative Physiology Part A* 187 (2001) 817-824.
- [3] R. E. Young, Correlated activities in the cardiorespirator nerves and ventilatory system in the norwegian lobster, *Nephrops norvegicus* (L.). *Comparative Biochemistry and Physiology Part A: Physiology* 61(1978) 387-394.
- [4] L. H. Field, J. L. Larimer, The cardiorespiratory system of crayfish: neuroanatomy and physiology. *Journal of Experimental Biology* 62 (1975) 519-530.
- [5] T. Yazawa, K. Kuwasawa, The cardio-respirator nerves of the hermit crabs: anatomical and electrophysiological identification of their distribution inside the heart. *Journal of Comparative Physiology Part A* 154 (1984) 871-881.
- [6] A service of the U.S. National Library of Medicine. <http://ghr.nlm.nih.gov/gene/NKX2-5> (accessed Sep 20 2014%).
- [7] C.-K. Peng, S. Havlin, H. E. Stanley, A. L. Goldberger, Quantification of scaling exponents and crossover phenomena in nonstationary heartbeat time series, *Chaos* 5 (1995) 82-87.
- [8] T. Yazawa, Crustacean stress behavior. In: T. Hariyama, T. Shimozawa (eds.) *Insect Mimetics. Advanced Biomimetics Series 3*, NTS, Tokyo, Japan (2008) 542-548 (in Japanese).
- [9] A. L. Goldberger, B. J. West, Application of nonlinear dynamics to clinical cardiology. *Annals of the New York Academy of Science* 504 (1987) 195-231.
- [10] A. A. Cecen, C. Erkal, Nonlinear dynamical modeling in ECG analysis: A heuristic guideline. *Nonlinear Dynamics, Psychology, and Life Sciences* 12 (2008) 359-369.
- [11] C.-K. Peng, S. Havlin, J. M. Hausdorff, J.E. Mietus, H.E. Stanley, A. L. Goldberger, Fractal mechanisms and heart rate control: Long-range correlations and their breakdown with disease. In: Rienzo M Di, et al. (eds.) *Frontiers of blood pressure and heart rate analysis*. IOS Press, Amsterdam, Netherlands (1997) 3-14.
- [12] L. Glass, Dynamical disease-The impact of nonlinear dynamics and chaos on cardiology and medicine. In: C. Grebogi et al. (eds.) *The impact of chaos on science and society*. United Nations University Press, Tokyo (1997) 219-231.
- [13] T. Stadnitski, Some critical aspects of fractality research. *Nonlinear Dynamics, Psychology, and Life Sciences* 16 (2012) 137-158.

- [14] H. E. Stanley, Phase transitions. Power laws and universality, *Nature* 378 (1995) 554.
- [15] T. Katsuyama, Scaling analysis of unstable fluctuation of heartbeat in spiny lobster. Numazu College of Technology Report 38 (2004) 189-194 (in Japanese).
- [16] O. B.-Perez, J. M. de Sa, J. L. R.-Alvarez, R. G.-Esteban, Changes in detrended fluctuation indices with aging in healthy and congestive heart failure subjects. *Computers in Cardiology*, 35 (2008) 45-48.
- [17] L. S. Liebovitch, T. Penzel, J. W. Kantelhardt, Physiological relevance of scaling of heart phenomena, In: A. Bunde et al. (eds) *The science of disasters: climate disruptions, heart attacks, and market crashes*, Springer (2002) p331-352.
- [18] H. V. Huikuri, T. H. Mäkikallio, C.-K. Peng, A.L. Goldberger, U. Hintze, M. Møller, Fractal correlation properties of R-R interval dynamics and mortality in patients with depressed left ventricular function after an acute myocardial infarction, *Circulation* 101 (2000) 47-53.
- [19] J. T. Bigger Jr, R. C. Steinman, L. M. Rolnitzky, J. L. Fleiss, P. Albrecht, R.J. Cohen, Power law behavior of R-R interval variability in healthy middle-aged persons, patients with recent acute myocardial infarction, and patients with heart transplants. *Circulation* 93 (1996) 2142-2151.
- [20] N. Scafetta, P. Grigolini, Scaling detection in time series: Diffusion entropy analysis. *Physical Review E* 66 (2002) 036130-1-10.